Interface effects in the Raman scattering of InN/AlN superlattices

E. F. Bezerra, E. B. Barros, J. R. Gonçalves, V. N. Freire, J. Mendes Filho, and V. Lemos*
Departamento de Física, Universidade Federal do Ceará, Centro de Ciências,
Caixa Postal 6030, Campus do Pici, 60455–900 Fortaleza, Ceará, Brazil
(Received 11 April 2002; published 24 October 2002)

Calculations of the Raman spectra of zinc blende InN/AlN superlattices were carried out assuming the existence of interface regions with thickness δ varying from zero to three monolayers. The optical branches were greatly affected by interfacing, while the acoustic branches remained practically unchanged. Frequency shifts up to 80 cm^{-1} were observed for some of the optical frequencies when $\delta=3$. The higher frequency peaks were observed to shift downward with increasing the interface thickness. Many peaks appearing at the low frequency side shift toward the center position of the spectrum. As a consequence, pairs of the Raman modes become quasidegenerate giving rise to highly prominent structures in the spectrum for $\delta=2$ and 3. Effects of localization of atomic displacements at the interface regions are shown.

DOI: 10.1103/PhysRevB.66.153314 PACS number(s): 68.90.+g, 63.20.Dj, 63.20.Pw

I. INTRODUCTION

The great interest of group III nitride semiconductors quantum well (QW) structures in the fabrication of optoelectronic devices is currently known.[1,2] The optical and electrical processes in GaN, AlN, and InN based QW and superlattice (SL) structures are remarkably influenced by the existence of interfaces. In GaAs/AlAs QW's, surface segregation leads to the generation of an atomic-scale disorder in the first overgrowth monolayers.[3,4] Several studies in GaAs/AlAs SL's suggest the need to consider interface effects in describing the optical phonon spectrum.[5,6] In addition to surface segregation the mismatch between the atomic radii of cations and anions is much larger in the nitrides. This aspect is of interest due to the increased disorder to result in wider interfaces. Actually, a typical interface width of 1 nm (2 nm) was measured for the GaN/InGaN (InGaN/AlGaN) interface.[7] For $GaN/Al_xGa_{1-x}N$ SL's, Raman measurements indicate interface thickness to be of the order of 2 nm.[8] Those values are much larger than the interface thicknesses found for the arsenide based SL's. Lattice dynamics calculations result in bulk phonon frequencies to be of use in the simulation of the Raman scattering.[9,10] Previous results show that interfacing effects are responsible for considerable gain in intensity of Raman modes in zinc blende GaN/AlN and GaN/InN SL's.[11,12] Even though the acoustic branch of bulk AlN overlap with the optical branch of InN, their optical dispersion curves do not overlap.[10,13] Therefore, it is interesting to analyze the interface dependence of optical phonons in the InN/AlN SL's.

Here, we calculate the phonon dispersion, atomic displacements and the Raman spectra of $(InN)_{8-\delta}/(InN_{0.5}AlN_{0.5})_\delta/(AlN)_{8-\delta}/(InN_{0.5}AlN_{0.5})_\delta$ SL's, with $\delta=1,2,3$. Most of the optical phonons were found to be confined in the abrupt SL probably as a consequence of nonoverlapping optical branches of bulk constituents. Strong localization of modes in the InN/AlN interfaced SL's results as a consequence of interfacing. The insertion of an interface and also accidental degeneracies of modes resulted in the Raman spectrum for $\delta=3$ to show a middle frequency peak with intensity comparable with those limiting the optical range.

II. RESULTS AND DISCUSSION

The present work employs a modified linear chain model with each atom representing a plane of atoms in the actual SL. Therefore, the associated phonons propagating along the [001] axis can be described through a one-dimensional set of equations of motion.[14,15] They can be solved in the harmonic approximation and the eigenvalues and eigenvectors are obtained by diagonalization of the dynamical matrix. The force constants were obtained considering interaction to nearest and next-nearest neighbors, only. Alloyed interfaces were considered to have one-mode-type behavior, based on previous demonstrations of this behavior for LO modes in other nitride alloys studied either experimentally,[16–20] or theoretically.[10,21,22] The bond-polarizability model,[14,15] which provides a good description of optical modes, was used to calculate the Raman spectra of the SL's. Symmetry arguments show that only the LO modes should contribute in the Raman backscattering geometry along [001] of a perfect superlattice constructed with zinc blende–type components.[15] The polarizability constants were assumed to have fixed values throughout the SL. The bulk InN and AlN mode frequencies and the force constants are listed in Table I. The frequencies were chosen as experimental values, when possible, or theoretical values in the lack of the former. Therefore, the AlN zone-center LO frequency was taken as 902 cm^{-1} from experimental data of Harima *et al.*[16] and the InN LO(Γ) frequency was taken as the value measured by using Raman scattering.[23] The acoustic LA(X) and LO(X) frequencies from the AlN dispersion relations reported by Karch *et al.*[24] Notice that those values are almost coincident

TABLE I. Bulk AlN and InN mode frequencies as used in the model to derive the force constants k, q_1, and q_2. The frequency values are in units of cm^{-1}.

	LO (Γ)	LO (X)	LA (X)	k (Nm^{-1})	q_1 (Nm^{-1})	q_2 (Nm^{-1})
AlN	902[a]	723[b]	594[b]	222.8	30.0	2.7
InN	588[c]	567[d]	231[d]	128.2	26.9	2.8

[a]From Ref. 16
[b]From Ref. 24
[c]From Ref. 23
[d]From Ref. 25

with the average between the two theoretical values listed in Table II of Ref. 25. We thus believe they are good input parameters for the present calculation. The remaining zone edge phonon frequencies for InN were obtained from the calculations of Bechstedt *et al.*[25] The aluminum molar fraction in the interfaced monolayers was taken as $x=0.5$. The force constants between atoms in the alloyed interface were taken as the average of those for the constituents.

The dispersion for the sharp interface (ideal) $(\mathrm{InN})_{n_1}/(\mathrm{AlN})_{n_2}$ SL, with $N=n_1+n_2$, is formed by N optical and N acoustic branches.[6] For $n_1=n_2=8$, the SL is expected to have 16 optical and 16 acoustic phonon branches. In this context the 32 vibrational modes will be referred to by numbers in order of increasing frequency. The branches for folded acoustic phonons were found to be highly dispersive for modes 1–10. The remaining six branches were nondispersive, as usually found for optical modes. This fact will be clarified further on when discussing atomic displacements.

For backscattering along the z axis ([001] direction), the Raman tensor can be expressed in terms of components of the differential polarizability tensor, α_{ij}, and the atomic displacements along z, u_{ij}, as[14]

$$\omega R_{xx}(\omega)\propto\left|\sum_A \alpha_{xx,A}(u_{1z}-u_{3z})\right|^2 \tag{1}$$

for modes of A_1 symmetry of the point group of the SL, or

$$\omega R_{xy}(\omega)\propto\left|\sum_A \alpha_{xy,A}(u_{1z}+u_{3z}-2u_{0z})\right|^2 \tag{2}$$

for modes of B_2 symmetry. The summations run over all A atoms (standing either for the indium or aluminum atom in the chain). Therefore, the atomic displacement factors in the above equations cannot vanish in order to result a contribution to the Raman intensity. It is also expected that superposition of accidentally degenerated modes should result in enhanced intensities. The symmetry properties are those of the zinc blende–type SL's grown along [001]. That is, it belongs either to the $P\bar{4}m2$ or $I\bar{4}m2$ depending on N being even or odd, respectively. In both cases, however, the point group is $\bar{4}m2$.[15]

Calculated Raman spectra for zinc blende $(\mathrm{InN})_{8-\delta}/(\mathrm{InN_{0.5}AlN_{0.5}})_\delta/(\mathrm{AlN})_{8-\delta}/(\mathrm{InN_{0.5}AlN_{0.5}})_\delta$ SL's are presented in Fig. 1 for several values of interface thickness δ. The lowest curve, for $\delta=0$, shows two dominant peaks at $\omega=585\ \mathrm{cm}^{-1}$ (due to modes 22 and 23 that have almost the same frequency) and $\omega=899\ \mathrm{cm}^{-1}$ (mode 32). The frequency of mode 32 is quasicoincident with the LO bulk value of AlN. In between, several weak structures appear at $\omega=669\ \mathrm{cm}^{-1}$ and $\omega=721\ \mathrm{cm}^{-1}$, $\omega=753\ \mathrm{cm}^{-1}$, $\omega=823\ \mathrm{cm}^{-1}$, and $\omega=874\ \mathrm{cm}^{-1}$ corresponding to modes 24, 25, 26, 28, and 30, respectively. This identification was made by comparison of the Raman frequencies with the values found in the calculated dispersion relations.

The introduction of an interface with $\delta=1$ results in a modified spectrum with an additional peak at $\omega=610\ \mathrm{cm}^{-1}$ (mode 23), and a down shift in frequency for the remaining features in the middle range of the spectrum

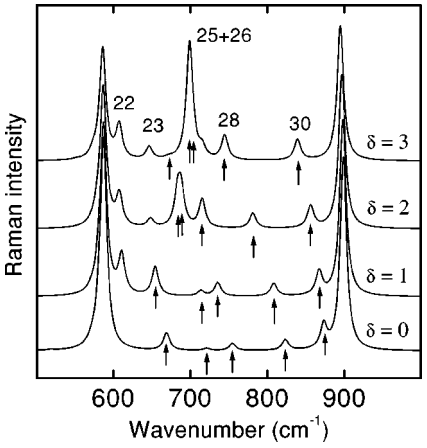

FIG. 1. Calculated Raman spectra for zinc blende $(\mathrm{InN})_{8-\delta}/(\mathrm{InN_{0.5}AlN_{0.5}})_\delta/(\mathrm{AlN})_{8-\delta}/(\mathrm{InN_{0.5}AlN_{0.5}})_\delta$ SL's. Arrows indicate the set of modes 24–26, 28 and 30. Numbers are for some of the most affected Raman modes for $\delta=3$.

[600,870] cm^{-1}. This is shown in Fig. 1 ($\delta=1$), where the arrows indicate modes 24, 25, 26, 28, and 30. A larger interface, of two monolayers causes further increase of the number of peaks in the middle frequency range, with the appearance of mode 22 at $\omega=607\ \mathrm{cm}^{-1}$. The same set of peaks as before is indicated by arrows in the spectrum labeled $\delta=2$ in Fig. 1. It can be noticed that the lower frequency peaks shift upward (related to $\delta=1$) while those of higher frequency shift downward, resulting in a more crowded middle range than in the case of $\delta=1$. Figure 1 also shows a remarkable increase of the Raman intensity, particularly in the spectra for $\delta=2$ at $\omega\simeq685\ \mathrm{cm}^{-1}$ and $\delta=3$ at $\omega\simeq698\ \mathrm{cm}^{-1}$. Notice that the new peak for $\delta=3$ is of the same magnitude as the end of range peaks. In order to associate the middle range features to predicted modes examination of the plot of ω versus number of modes can be of help. Figure 2 shows such a plot, including all the optical phonons. The open symbols

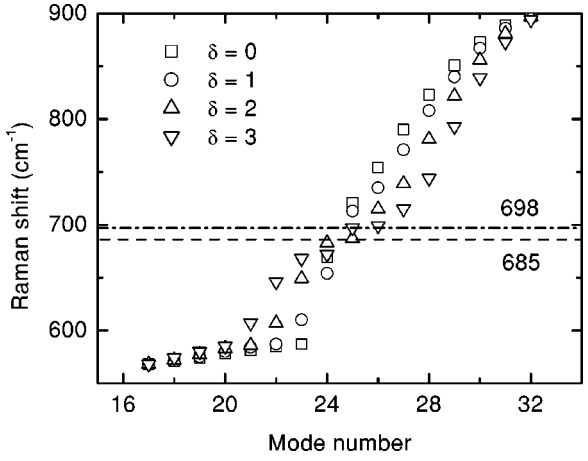

FIG. 2. Frequency versus $(\mathrm{InN})_{8-\delta}/(\mathrm{InN_{0.5}AlN_{0.5}})_\delta/(\mathrm{AlN})_{8-\delta}/(\mathrm{InN_{0.5}AlN_{0.5}})_\delta$ SL's optical mode numbers. The dashed line was drawn at the average between the frequencies of the modes 24 and 25 for $\delta=2$. The dot-dashed line represent average of the frequencies of modes 25 and 26 for $\delta=3$.

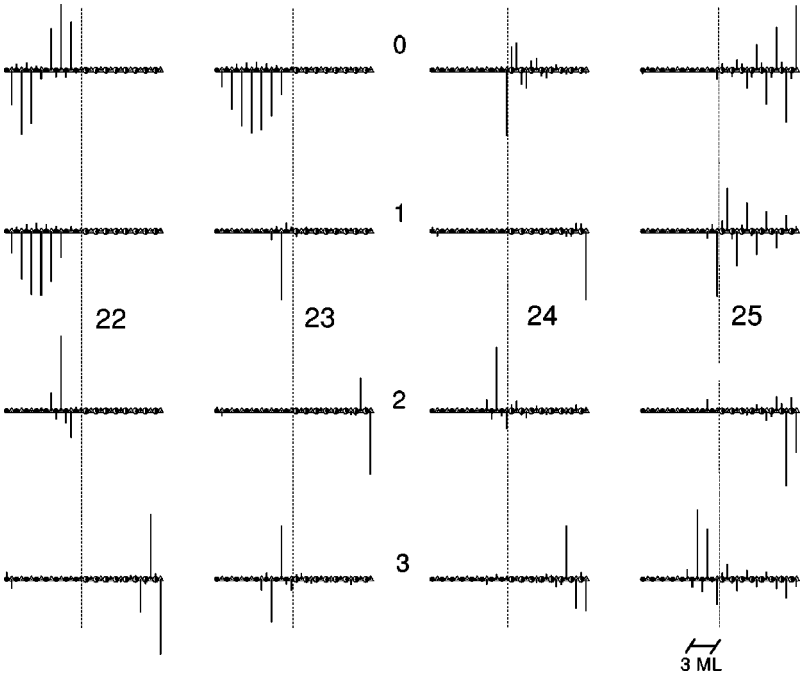

FIG. 3. Magnitude of atomic displacements of selected optical modes for the $(InN)_{8-\delta}/(InN_{0.5}AlN_{0.5})_{\delta}/(AlN)_{8-\delta}/(InN_{0.5}AlN_{0.5})_{\delta}$ SL's with $\delta=0$, 1, 2, and 3. Triangles stand for N and full circles for In atoms. Al atoms are represented by the biggest circles. The numbers in the horizontal line indicate the mode selected and those in the vertical line are for the interface thickness.

indicate the four values of interface width. The dashed line was traced coincident with the dominant middle range feature of the Raman spectrum for $\delta=2$, and the dot-dashed line with that feature of the Raman spectrum for $\delta=3$. It is seen in Fig. 2 that the latest lines cross two symbols each. The crossing illustrate the occurrence of quasidegenerate modes 24, 25 for $\delta=2$ and 25, 26 for $\delta=3$. This is probably one of the reasons why those peaks are so intense. It should be noted that the symbols in Fig. 2 are spread for modes 21 to 31, but not for modes 16 to 20 or the mode 32. This indicates that the unchanged frequencies correspond to vibrations less affected by interfacing. Those with important frequency shifts, modes 22, 23, 26–29, are greatly affected by interfacing and some of them contribute with structures in the middle frequency range of the Raman spectrum.

The atomic displacements were calculated for all vibrations. The lowest frequency ($\omega<231$ cm^{-1}) modes, numbered 1–10, were found to propagate through the whole superlattice. Acoustic phonons with frequency in the range [290,520] cm^{-1}, corresponding to modes 11–15, have atomic vibrations confined in the AlN layers. The acoustic mode 16, with frequency above 567 cm^{-1}, is also extended. Interfacing does not change this situation appreciably. The acoustic phonons behaving as confined modes may, in principle, cause some surprise. But, by examining the dispersion relation of the bulk constituents, it is seen that the AlN acoustic branch does not overlap the InN acoustic branch in the [290,520] cm^{-1} frequency range, thus producing confinement in this range. On the other hand, the AlN acoustic branch overlap the InN optical branch above 567 cm^{-1} close to the Brillouin zone *X* point, thus causing extended behavior of mode 16. This is in contrast with previous observations of acoustic mode behavior in AlN/GaN or GaN/InN superlattices.[11,12] The acoustic phonons are not being detailed any longer, due to the fact that the present treatment is not recommended for them.[15]

Most of the optical modes were found to be confined either in the InN layers or in the AlN layers for $\delta=0$. Modes 17 and 18 are exceptions, being extended for $\delta=0$. The extension of those optical modes is related to the overlapping of the InN optical branch with the AlN acoustic branch close to the Brillouin zone limit of the bulk constituents. A similar behavior has been observed before for AlN/GaN SL's,[11] caused by overlapping of optical branches. Modes 19 to 23 are confined to the InN layers and the remaining modes to the Al*N* layers, except for the mode 24 that is well localized at the InN/AlN interface for $\delta=0$ (see Fig. 3).

Confinement of modes 25 to 32 are observed for $\delta=1$. Interfacing was observed to produce localization of the modes to a certain extent. To better appreciate this effect the amplitude of atomic displacements are plotted in Fig. 3, for modes selected among those that localize upon interfacing. For $\delta=1$ the mode 23 is found to localize at the direct InN/AlN interface; for $\delta=2$ it localizes at the inverse AlN/InN interface, and for $\delta=3$ it localizes back at the direct interface. The mode 24 behaves in an inverted way, localizing at the opposed interfaces. Both modes loose, to a certain degree, the localized character for $\delta=3$. They contribute to the Raman intensity particularly for $\delta=1$ and $\delta=2$. Mode 25 is well localized at the inverse interface at $\delta=2$ and less localized at the direct interface for $\delta=3$. Mode 26 shows atomic displacements close to both interfaces for $\delta=3$. Their contribution to the Raman intensity gives rise to an important structure in the spectrum.

Comparison with experiment is lacking because this kind of superlattice of the cubic nitrides is not yet available. Just recently some data on the phonon properties of low-dimensional III-nitrides appeared, but they are restricted to systems based on GaN and AlN of the hexagonal structures.[26–28] It should be mentioned at this point that if the calculated spectra will be compared with experiments the

effect of strain has to be considered. The in-plane strain depend on the structure of the SL and growth conditions. It can be measured, for instance, using optical spectroscopy.[29] The values of strains allow for the determination of induced frequency shifts that correct the input parameters of the program. The shifts depend also on the phonon deformation potentials and elastic properties. The deformation potentials are published for AlN in the wurtzite modification[30] but those for InN are still lacking. Therefore, a complete analyzes of strain effects in this type of SL has to be postponed at present.

III. CONCLUSION

Summarizing, the interface effects on the Raman spectra of zinc blende $(InN)_{8-\delta}/(InN_{0.5}AlN_{0.5})_{\delta}/(AlN)_{8-\delta}/(InN_{0.5}AlN_{0.5})_{\delta}$ SL's were studied using a linear chain description and the bond-polarizability model. It is shown that the optical modes region of the spectrum is severely affected by the existence of graded interface regions. The main influence is the increase of the Raman intensity of peaks located in between those related to the end spectra modes. These peaks tend to shift with increasing δ toward the center position in the spectrum. The $\delta=3$ interface effects in the Raman intensities are drastic, giving rise to a most prominent structure in the middle frequency range of the spectrum. This structure results from the overlap of two quasi–degenerate modes. Examination of atomic displacements allowed for observation of the effects of interfacing to generate localization of the vibrations. These effects are much stronger than those observed previously for other SL's based on III-V or Si/Ge constituents. The optical modes are, therefore, well suited as a probe for interfacing with both frequency and Raman intensity, highly affected.

ACKNOWLEDGMENTS

The authors acknowledge financial support from Fundação de Amparo à Pesquisa do Estado do Ceará (FUNCAP) and the Conselho Nacional de Desenvolvimento Científico e Tecnológico (CNPq). Two of us, V.L. and V.N. F., are thankful to CNPq for partial support through grant for ''NanoSemiMat'' (Grant No. 550.015/01-9).

*Email address: volia@fisica.ufc.br

[1] S. Nakamura, Semicond. Sci. Technol. **14**, R27 (1999); *The Blue Laser Diode–GAN Based Light Emitters and Lasers* (Springer, Berlin, 1997).
[2] F.A. Ponce and D.P. Bour, Nature (London) **386**, 351 (1997).
[3] K. Leosson, J.R. Jensen, W. Langbein, and J.M. Hvam, Phys. Rev. B **61**, 10 322 (2000).
[4] V. Lemos, C.S. Sérgio, A.P. Lima, A.A. Quivy, R. Enderlein, J.R. Leite, and W. Carvalho, Jr., Radiat. Eff. Defects Solids **146**, 187 (1998), and references therein.
[5] K.T. Tsen, J. Raman Spectrosc. **27**, 277 (1996); K.T. Tsen, D.J. Smith, S.C.Y. Tsen, N.S. Kumar, and H. Morkoç, J. Appl. Phys. **70**, 418 (1991).
[6] B. Samson, T. Dumelow, A.A. Hamilton, T.J. Parker, S.R.P. Smith, D.R. Tilley, C.T. Foxon, D. Hilton, and K.J. Moore, Phys. Rev. B **46**, 2375 (1992).
[7] C. Kisielowski, Z. Liliental-Weber, and S. Nakamura, Jpn. J. Appl. Phys. **36**, 6932 (1997).
[8] D. Behr, R. Niebuhr, J. Wagner, K.-H. Bachem, and U. Kaufmann, Appl. Phys. Lett. **70**, 363 (1997).
[9] G. Kaczmarczyk, A. Kaschner, S. Reich, A. Hoffmann, C. Thomsen, D.J. As, A.P. Lima, D. Schikora, K. Lischka, R. Averbeck, and H. Riechert, Appl. Phys. Lett. **76**, 2122 (2000).
[10] F. Bechstedt and H. Grille, Phys. Status Solidi B **216**, 761 (1999).
[11] E.F. Bezerra, V.N. Freire, A.M.R. Teixeira, M.A. Araújo Silva, P.T.C. Freire, J. Mendes Filho, and V. Lemos, Phys. Rev. B **61**, 13 060 (2000).
[12] E.F. Bezerra, A.G. Souza Filho, V.N. Freire, J. Mendes Filho, and V. Lemos, Phys. Rev. B **64**, 201306 (2001).
[13] C. Bungaro, K. Rapcewicz, and J. Bernholc, Phys. Rev. B **61**, 6720 (2000).
[14] B. Zhu and K.A. Chao, Phys. Rev. B **36**, 4906 (1987).
[15] B. Jusserand and M. Cardona, in *Light Scattering in Solids V*, edited by M. Cardona and G. Güntherodt, Vol. 66 of *Topics in Applied Physics* (Springer, Heidelberg, 1989), p. 49.
[16] H. Harima, T. Inoue, S. Nakahima, O. Okumura, T. Ishida, S. Yoshida, T. Koizumi, H. Grille, and F. Bechstedt, Appl. Phys. Lett. **74**, 191 (1999).
[17] A. Tabata, J.R. Leite, A.P. Lima, E. Silveira, V. Lemos, T. Frey, B. Schöttker, D. Schikora, and K. Lischka, Appl. Phys. Lett. **75**, 1095 (1999).
[18] E. Silveira, A. Tabata, J.R. Leite, R. Trentin, V. Lemos, T. Frey, D.J. As, D. Schikora, and K. Lischka, Appl. Phys. Lett. **75**, 3602 (1999).
[19] T. Inushima, T. Shiraishi, and V.Y. Davydov, Solid State Commun. **110**, 491 (1999).
[20] M.S. Liu, Y.Z. Tong, Les A. Bursill S. Prawer, K.W. Nugent, and G.Y. Zhang, Solid State Commun. **108**, 765 (1998).
[21] H. Grille and F. Bechstedt, J. Raman Spectrosc. **27**, 201 (1996).
[22] D.N. Tawar, Mater. Sci. Eng., B **47**, 155 (1997).
[23] A. Tabata, A.P. Lima, L.K. Teles, L.M.R. Scolfaro, J.R. Leite, V. Lemos, B. Schöttker, T. Frey, D. Schikora, and K. Lischka, Appl. Phys. Lett. **74**, 362 (1999).
[24] K. Karch and F. Bechstedt, Phys. Rev. B **56**, 7404 (1997).
[25] F. Bechstedt, U. Grossner, and J. Furthmüller, Phys. Rev. B **62**, 8003 (2000).
[26] J. Gleise, J. Frandon, F. Damangeot, M.A. Renucci, M. Kuball, J.M. Hayes, F. Widmann, and B. Daudin, Mater. Sci. Eng., B **82**, 27 (2001).
[27] L. Bergman, M. Dutta, M.A. Stroscio, S.M. Komirenko, R.J. Nemanich, C.J. Eiting, D.J.H. Lambert, H.K. Kwon, and R.D. Dupuis, Appl. Phys. Lett. **76**, 1969 (2000).
[28] S.M. Komirenko, K.W. Kim, M.A. Stroscio, and M. Dutta, Phys. Rev. B **59**, 5013 (1999).
[29] C.K. Inoki, V. Lemos, F. Cerdeira, and C. Vásquez-López, J. Appl. Phys. **73**, 3266 (1993).
[30] J.-M. Wagner and F. Bechstedt, Appl. Phys. Lett. **77**, 346 (2000).